JACS
JOURNAL OF THE AMERICAN CHEMICAL SOCIETY

ARTICLE

pubs.acs.org/JACS

Photoreduction of ^{99}Tc Pertechnetate by Nanometer-Sized Metal Oxides: New Strategies for Formation and Sequestration of Low-Valent Technetium

Benjamin P. Burton-Pye,[†] Ivana Radivojevic,[†] Donna McGregor,[†,‡] Israel M. Mbomekalle,[†,∥] Wayne W. Lukens, Jr.,[§] and Lynn C. Francesconi*[,†,‡]

[†]Department of Chemistry, Hunter College of the City University of New York, 695 Park Avenue, New York, New York 10065, United States

[‡]Department of Chemistry, Graduate Center of the City University of New York, 365 Fifth Avenue, New York, New York 10016, United States

[§]Chemical Sciences Division, The Glenn T. Seaborg Center, E.O. Lawrence Berkeley National Laboratory (LBNL), One Cyclotron Road, Berkeley, California 94720, United States

Supporting Information

ABSTRACT: Technetium-99 (^{99}Tc) (β^-_{max}: 293.7 keV; $t_{1/2}$: 2.1 × 10^5 years) is a byproduct of uranium-235 fission and comprises a large component of radioactive waste. Under aerobic conditions and in a neutral−basic environment, the pertechnetate anion ($^{99}TcO_4^-$) is stable. $^{99}TcO_4^-$ is very soluble, migrates easily through the environment and does not sorb well onto mineral surfaces, soils, or sediments. This study moves forward a new strategy for the reduction of $^{99}TcO_4^-$ and the chemical incorporation of the reduced ^{99}Tc into a metal oxide material. This strategy employs a single material, a polyoxometalate (POM), α_2-$[P_2W_{17}O_{61}]^{10-}$, that can be photoactivated in the presence of 2-propanol to transfer electrons to $^{99}TcO_4^-$ and incorporate the reduced ^{99}Tc covalently into the α_2-framework to form the $^{99}Tc^VO$ species, $^{99}Tc^VO(\alpha_2\text{-}P_2W_{17}O_{61})^{7-}$. This occurs via the formation of an intermediate species that slowly converts to $^{99}Tc^VO(\alpha_2\text{-}P_2W_{17}O_{61})^{7-}$. Extended X-ray absorption fine structure and X-ray absorption near-edge spectroscopy analysis suggests that the intermediate consists of a ^{99}Tc(IV) α_2- species where the ^{99}Tc is likely bound to two of the four W−O oxygen atoms in the α_2-$[P_2W_{17}O_{61}]^{10-}$ defect. This intermediate then oxidizes and converts to the $^{99}Tc^VO(\alpha_2\text{-}P_2W_{17}O_{61})^{7-}$ product. The reduction and incorporation of $^{99}TcO_4^-$ was accomplished in a "one pot" reaction using both sunlight and UV irradiation and monitored as a function of time using multinuclear nuclear magnetic resonance and radio thin-layer chromatography. The process was further probed by the "step-wise" generation of reduced α_2-$P_2W_{17}O_{61}^{12-}$ through bulk electrolysis followed by the addition of $^{99}TcO_4^-$. The reduction and incorporation of ReO_4^-, as a nonradioactive surrogate for ^{99}Tc, does not proceed through the intermediate species, and Re^VO is incorporated quickly into the α_2-$[P_2W_{17}O_{61}]^{10-}$ defect. These observations are consistent with the periodic trends of ^{99}Tc and Re. Specifically, ^{99}Tc is more easily reduced compared to Re. In addition to serving as models for metal oxides, POMs may also provide a suitable platform to study the molecular level dynamics and the mechanisms of the reduction and incorporation of ^{99}Tc into a material.

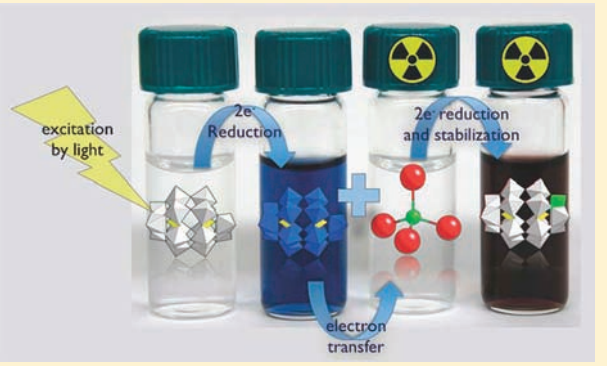

INTRODUCTION

Technetium-99 (^{99}Tc) comprises a large component of radioactive waste found in waste tanks at Hanford and Savannah River as well as water and soil samples around national laboratory sites in the United States. The chemistry of ^{99}Tc suggests that under aerobic conditions and in a basic environment, the stable heptavalent pertechnetate anion ($^{99}TcO_4^-$) predominantly exists. This oxyanion is the most thermodynamically stable form of technetium at high pH.[1] It is very soluble, migrates easily through the environment and does not sorb well onto mineral surfaces, soils, or sediments.[1−10] The long half-life of ^{99}Tc (2.1×10^5 years) and the high environmental mobility of the pertechnetate anion create a particular concern when trying to develop waste remediation strategies.

One of the most commonly considered potential strategies for ^{99}Tc remediation is focused on pertechnetate reduction. The mobile pertechnetate ion can be removed from solution by reduction to insoluble, low-valent $^{99}Tc^{IV}$ species (such as $^{99}TcO_2 \cdot nH_2O$), which can then be physically adsorbed to a

Received: June 30, 2011
Published: October 10, 2011

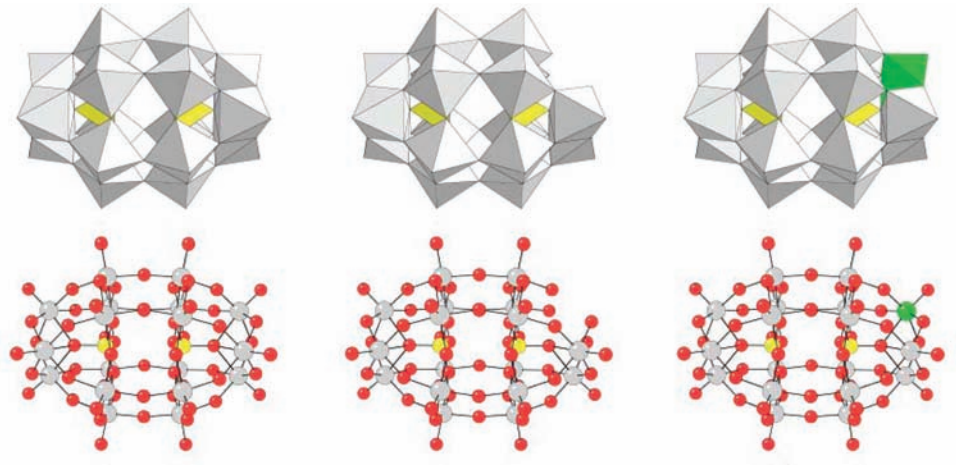

Figure 1. Polyhedral (top) and ball and stick (bottom) structural representations of the parent plenary Wells–Dawson ion; α-$[P_2W_{18}O_{62}]^{6-}$ (left), monovacant lacunary α_2-$[P_2W_{17}O_{61}]^{10-}$ (center), and the complex $^{99}Tc^{V}/Re^{V}O(\alpha_2$-$P_2W_{17}O_{61})^{7-}$ (right). Phosphorus atoms are represented in yellow, tungsten atoms are shown in white, oxygen atoms shown are in red, and technetium is represented in green. Upon removal of a $(W{=}O)^{3+}$ unit from the "cap" region, a defect site is formed in the monovacant α_2-$[P_2W_{17}O_{61}]^{10-}$isomer. The four O atoms of the vacancy can bind to ^{99}Tc and Re ions. The metal ions (W, ^{99}Tc, or Re) are contained within the octahedra, each bound to one terminal oxygen and four bridging oxygen atoms and associated with one oxygen from the phosphate moiety.

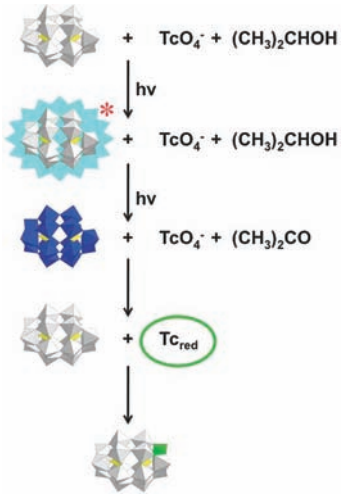

Figure 2. General strategy for photolytic reduction of $^{99}TcO_4^-$ by α_2-$[P_2W_{17}O_{61}]^{10-}$. The α_2-$[P_2W_{17}O_{61}]^{10-}$ POM (white polyhedra) is promoted to an excited state by irradiation, whereupon the excited POM is reduced by a sacrificial electron donor to the "reduced" α_2-$[P_2W_{17}O_{61}]^{12-}$ (blue polyhedra). The reduced α_2-$[P_2W_{17}O_{61}]^{12-}$ transfers electrons to $^{99}TcO_4^-$, resulting in reduction to low-valent ^{99}Tc (green octahedron) that will be incorporated into the lacunary POM as the $^{99}Tc^{V}{=}O$ species.

solid surface or mixed within glass, cement, or ceramic. It has been shown that physical mixing of $^{99}TcO_2$ with these materials ultimately results in oxidation of the $^{99}Tc^{IV}$ to $^{99}Tc^{VII}O_4^-$.[11]

Bioimmobilization efforts have also been employed in the efforts to reduce and stabilize $^{99}TcO_4^-$ in soil by natural organic matter.[8,12] In these studies chemical reduction[7,13] and microbial reduction[5,14] led to the formation of $^{99}TcO_2 \cdot nH_2O$. However, the reduced $^{99}Tc^{IV}$ in the form of amorphous oxides also reoxidizes back to the mobile $^{99}Tc^{VII}O_4^-$ anion.[6]

Taking a cue from radiopharmaceutical chemistry, that employs the tracer isotope of technetium, ^{99m}Tc may provide a new strategy for reduction of pertechnetate and covalent chemical incorporation of the reduced ^{99}Tc into a material. In typical radiopharmaceutical "kits", ^{99m}Tc, as pertechnetate, $^{99m}TcO_4^-$, is reduced by stannous ion in the presence of coordinating ligands, and the low valent ^{99m}Tc covalently bonds to the ligands forming a ^{99m}Tc coordination complex.

In fact, this approach has been presented in a preliminary communication describing the reduction of $^{99}TcO_4^-$ and incorporation into a stannous phosphate material.[15] A similar study employed amorphous FeS for reduction of $^{99}TcO_4^-$ and binding of the reduced ^{99}Tc to the Fe–S material as probed by X-ray absorption near-edge spectroscopy (XANES), extended X-ray absorption fine structure (EXAFS), FT-IR, and energy dispersive X-ray spectroscopy (EDS). The $^{99}TcO_4^-$–FeS reductive immobilization reaction product was found to be predominantly $^{99}TcO_2$.[4]

Herein we move this approach forward taking advantage of the chemistry of the element. We identify a metal oxide system that can serve as both a reducing agent for the reduction of $^{99}TcO_4^-$ as well as a host that binds covalently to the reduced ^{99}Tc species. This new strategy employs a single material, a polyoxometalate (POM), both as the reducing agent and the coordinating ligand. Moreover, we can identify the final reduced ^{99}Tc product on the molecular level, and we can begin to understand the mechanism of the process.

POMs are polyanionic aggregates of early transition metals (Mo^{VI} and W^{VI}) and are strong, tunable electron donors to substrates.[16–22] POMs undergo stepwise, multielectron redox reactions while maintaining their structural integrity. They can be reversibly reduced through a variety of methods, including photochemical reduction,[22–32] reduction by γ radiolysis[33] in the presence of a sacrificial organic electron donor, electrochemical reduction, and chemical reduction using appropriate reducing agents.[34]

Due to their multielectron redox properties, reduced POMs, especially Keggin ions, have been used for the reduction of metal ions such as Ag^+, Pd^{2+}, Au^{III}, Pt^{IV}, and Cu^{2+} in aqueous systems

to lower oxidation states or to their metallic state.[17−20,25,26,35−37] The tunable redox nature and facile electron-transfer properties of POMs render them suitable materials for the synthesis of colloidal metal nanoparticles that are stabilized by the reoxidized POMs.[19,37−39]

While most of the published POM photocatalysis studies employ the "plenary" or parent POMs (Lindqvist, Keggin, Wells−Dawson), this study focuses on using the "lacunary" or defect Wells−Dawson isomer, α_2-$[P_2W_{17}O_{61}]^{10-}$. Figure 1 shows the parent Wells−Dawson ion, α-$[P_2W_{18}O_{62}]^{6-}$, and the α_2-$[P_2W_{17}O_{61}]^{10-}$ isomer that is formed by removal of a W^{VI}═O from the "cap" region. This α_2-$[P_2W_{17}O_{61}]^{10-}$ species possesses a site wherein four oxygen atoms can bind to a metal ion, such as a reduced ^{99}Tc, depicted in Figure 1.

We hypothesize that the α_2-$[P_2W_{17}O_{61}]^{10-}$ can not only transfer electrons to $^{99}TcO_4^-$ but can also incorporate the reduced ^{99}Tc covalently into the α_2- framework to form the $^{99}Tc^{V}O$ species, $^{99}Tc^{V}O(\alpha_2\text{-}P_2W_{17}O_{61})^{7-}$. We can then compare the $^{99}Tc^{V}O(\alpha_2\text{-}P_2W_{17}O_{61})^{7-}$ synthesized via this approach with the chemically synthesized complex that we recently reported.[40] A general mechanism for this procedure, shown in Figure 2, will be addressed in detail in the ensuing sections.

In this study, we also evaluate the reduction of ReO_4^- by photoactivation of α_2-$[P_2W_{17}O_{61}]^{10-}$. Re is often considered a nonradioactive surrogate for ^{99}Tc. This practice should be used with caution because the reduction potentials, kinetics, and even coordination environments can be different between these second- and third-row congeners. Performing studies with both ^{99}Tc and Re provides the opportunity to compare the chemistry, speciation, and fundamental differences between these two elements[40−42] and also allows for a more detailed understanding of the POM speciation.

EXPERIMENTAL SECTION

General. ^{99}Tc, a weak β-emitter (^{99}Tc: β_{max}: 0.29 MeV; $t_{1/2}$: 2.1 × 10^5 years) was obtained from Oak Ridge National Laboratory (as NH_4TcO_4). $^{188}ReO_4^-$ (^{188}Re: β_{max}: 2.12 MeV; γ: 155 keV (8%); $t_{1/2}$: 16.9 h) was eluted from a ^{188}W−^{188}Re generator that was obtained from Oak Ridge National Laboratory. All reported ^{99}Tc and ^{188}Re manipulations were performed in an appropriately equipped laboratory approved for the use of low-level radioactivity. Suitable radioactive material handling procedures were employed throughout.

All materials were purchased as reagent grade and used without further purification. Pure water was used throughout and was obtained using a Millipore Direct Q5 system (conductivity = 18 MΩ). Solid ammonium pertechnetate (NH_4TcO_4) was treated with H_2O_2 to oxidize any reduced forms of ^{99}Tc.[43] Standardization of prepared aqueous NH_4TcO_4 solutions was conducted according to an established UV−vis procedure.[43,44] POMs, $K_{10}(\alpha_2\text{-}P_2W_{17}O_{61})$ (***α2***),[45] $K_{7-n}H_n[Tc^{V}O\text{-}(\alpha_2\text{-}P_2W_{17}O_{61})]$ (**$^{99}Tc^{V}O$-*α2***),[40] and $K_{7-n}H_n[Re^{V}O(\alpha_2\text{-}P_2W_{17}O_{61})]$ (**$Re^{V}O$-*α2***)[46] were synthesized using literature procedures. All UV−vis data were collected on a Varian Cary 50 UV−vis spectrophotometer at 300 K.

Collection of NMR Data. Nuclear magnetic resonance (NMR) data were collected on a JEOL GX-400 spectrometer with 5 mm tubes fitted with Teflon inserts that were purchased from Wilmad Glass. The resonance frequency for ^{31}P and ^{99}Tc is 161.8 and 90.0 MHz, respectively, on this spectrometer. Chemical shifts are given with respect to external 85% H_3PO_4 for ^{31}P and 0.5 M NH_4TcO_4 for ^{99}Tc (the more negative chemical shifts denote upfield resonances). Typical acquisition parameters for ^{31}P spectra included the following: spectral width, 10 kHz; acquisition time, 0.8 s; pulse delay, 1 s; and pulse width, 15 μs (50° tip angle). For ^{99}Tc: spectral width, 9 kHz; acquisition time, 0.9 s; pulse delay 0.5 s; and pulse width, 10 μs (50° tip angle). Typically, between 200 and 2000 scans were acquired for ^{99}Tc and ^{31}P, respectively. For all spectra, the temperature was controlled to ±0.2°.

Collection of Electrochemical Data. Electrochemical data were obtained using a BASi voltammetric analyzer system controlled by BASi CV-50W software (for PC). The one-compartment cell used for cyclic voltammetry (CV) contained a glassy-carbon working electrode (BASi MF-2012 standard disk electrode, 3 mm OD), a Pt wire auxiliary electrode (0.5 mm), and a Ag/AgCl reference electrode (BASi MF-2052). Prior to obtaining electrochemical data, solutions were deaerated for at least 30 min with high purity Ar. A positive pressure of Ar was maintained during subsequent work. Preparation, including fine polishing of the glassy-carbon working electrode was adapted from the procedure of Keita and co-workers.[47] Unless indicated otherwise, scan rates were 10 mVs^{-1}, and all experiments were carried out at ambient temperature under an atmosphere of Ar. Electrochemical reduction was achieved using bulk electrolysis in a BASi bulk electrolysis cell. The working electrode was a reticulated vitreous carbon cage (BASi MF-2077), the auxiliary electrode was a platinum wire separated from the bulk electrolyte solution via a fritted compartment, and the reference electrode was Ag/AgCl (BASi MF-2052).

Radio Thin Layer Chromatography. Radio thin-layer chromatography (TLC) was performed on a radio TLC Imaging Scanner Bioscan Ar-2000. Quantitation of peaks is automatically performed, providing the percent of total activity for each peak. Chromatography paper (Whatman, 3MM CHR) was cut into 1 × 10 cm strips. Three μL of sample was spotted onto each TLC strip and developed in a 0.9% saline solvent system.[48] Radio TLC monitors the β emission of the ^{99}Tc and both the β and γ emissions of the ^{188}Re. This technique is thus species specific for ^{99}Tc and ^{188}Re containing compounds. Control experiments were performed to determine that, when eluted with saline, both $^{99}TcO_4^-$ and $^{188}ReO_4^-$ move with the solvent front (Supporting Information) and chemically synthesized **K-$^{99}Tc^{V}O$-*α2***[40] remains at the origin (Figure S1, Supporting Information).

Stability of $K_{10}(\alpha_2\text{-}P_2W_{17}O_{61})$ (*α2*) at Low pH As a Function of Concentration. The reduction of $^{99}TcO_4^-$ to low-valent states is favored at low pH.[49,50] While Keggin ions are known to be extremely stable at low pH,[21] the stability of ***α2*** at low pH has not been fully investigated. ^{31}P NMR data of the ***α2*** POM dissolved in a 3:1 mixture of 0.5 M H_2SO_4 (pH of 0.33):D_2O over time show that the POM stability is concentration dependent (Figure S2, Supporting Information). The more concentrated solutions (30 mM) resulted in large amounts of decomposition to the plenary α-$[P_2W_{18}O_{62}]^{6-}$ over the period of one week, while lower concentrations (4, 8, and 16 mM) showed only minimal amounts of decomposition during this time frame. The latter were thus chosen for the photoreduction experiments. (For photoreduction of $^{99}TcO_4^-$ by sunlight, a concentration of 32 mM ***α2*** was also employed and, as expected, decomposition to α-$[P_2W_{18}O_{62}]^{6-}$ occurred). A 5 mM concentration of ***α2*** was used for the bulk electrolysis experiments; in addition to minimized decomposition, the low concentration of POM is convenient for the operation of the electrolysis instrumentation.

Preparation of Samples for Reduction of $^{99}TcO_4^-$ and ReO_4^-. Three methods were employed to monitor the reduction of MO_4^- (where M = ^{99}Tc or Re). For most of the reductions, a stock solution of 0.28 M MO_4^- was used in a 1.2− 1.4 molar excess. For experiments involving the tracer isotope ^{188}Re, 500 μL of "cold" stock (0.28 M) ReO_4^- solution was spiked with 1 μL of 9 $\mu Ci\mu L^{-1}$ of $^{188}ReO_4^-$. Reduction solutions were prepared by mixing 0.5 M H_2SO_4:2-propanol:D_2O in a 2:1:1 volume ratio. Reduction solutions containing electrolyte were prepared by mixing 0.5 M of H_2SO_4 (containing 0.5 M Na_2SO_4):2-propanol:D_2O in a 2:1:1 volume ratio.

Method 1: In situ Reduction by UV Irradiation. Three different solutions were prepared by dissolving 50, 100, and 200 mg of **α2** (0.01, 0.02, and 0.04 mmol, respectively) in 2.5 mL of reduction solution (with and without electrolyte) and mixed thoroughly. This resulted in 4, 8, and 16 mM POM solutions, respectively. Each solution was placed in a quartz luminescence cuvette (path length, 10 mm). Standardized MO_4^- (0.28 M) was added in a slight molar excess (50 μL for 50 mg of POM, 90 μL for 100 mg, and 170 μL for 200 mg). The cuvettes were then sealed with a rubber septum, and the solutions purged with N_2 for 30 min before irradiation with a UV lamp at 254 nm (power @ 5 cm from source = 17.9 @ 200 μW) for 16 h and up to 24 h. After the irradiation periods, the colorless solutions changed to either light or dark red-brown in the case of ^{99}Tc or to a light or dark purple color in the case of Re. Each experiment was conducted using $^{99}TcO_4^-$, nonradioactive ("cold") ReO_4^-, and nonradioactive ReO_4^- spiked with ("hot") $^{188}ReO_4^-$. The samples were characterized with ^{31}P NMR and ^{99}Tc NMR and, in some cases, UV−vis and radio TLC paper chromatography where applicable.[48]

In these experiments 2-propanol was chosen as the sacrificial electron donor because it is known to be an effective photoreducing agent (through formation of a $(CH_3)_2COH$ hydroxyalkyl radical that can be easily oxidized to acetone)[51] and has been used extensively to aid in the reduction of $(PW_{12}O_{40})^{3-}$, $(SiW_{12}O_{40})^{4-}$, and $(P_2Mo_{18}O_{62})^{6-}$.[17−19,23,25,26]

To test a 1:1 **α2**:$^{99}TcO_4^-$ stoichiometry, the **α2** (57.9 mg, 11.6 μmol) was dissolved in 2.5 mL of reduction solution (with and without electrolyte) and mixed thoroughly. This resulted in a 4 mM POM solution. The solution was processed as described above and irradiated. After the irradiation, the colorless solutions changed to a light green/red after 19 h and a more intense red after 24 h. For the 19 h irradiation, ^{31}P NMR was taken immediately after irradiation was ceased and at timed intervals after irradiation was ceased. KCl (500 μL of a saturated solution) was added to the reaction solution directly through the septum via a syringe and the sample placed in the refrigerator overnight. The crystalline solid that formed (57 mg) was isolated by filtration. The solid was consequentially used for ^{31}P NMR and radio TLC.

Method 2: Electrochemically Reduced K_{10}(α2-$P_2W_{17}O_{61}$) (α2). In a 0.5 M H_2SO_4 (containing 0.5 M Na_2SO_4):D_2O mixture (1:1 vol, 20 mL), 500 mg (0.1 mmol) of **α2** was dissolved, resulting in a 5 mM **α2** solution. This solution was placed in an electrolysis cell and purged with argon for 30 min. A potential of −220 mV was applied via the working electrode to reduce the POM by 2 electrons. Upon applying the potential, the clear colorless solution immediately became deep blue. A slight excess of nitrogen purged 0.28 M MO_4^- (M = ^{99}Tc, Re) solution (500 μL, 1.4 equiv) was quickly added to the solution of electrochemically reduced **α2**, and a slow color change from dark blue to dark brown-red was observed in the case of ^{99}Tc, and from dark blue to dark purple in the case of Re. Each experiment was conducted using ^{99}Tc and "cold" Re. The reduction of MO_4^- was monitored via ^{31}P NMR and radio TLC in the case of ^{99}Tc.

Method 3: In situ Reduction by Sunlight. Four different solutions were prepared by dissolving 50, 100, 200, and 400 mg of **α2** (0.01, 0.02, 0.04, and 0.08 mmol, respectively) in a 2.5 mL mixture of reduction solution and mixed thoroughly. This resulted in 4, 8, 16, and 32 mM POM solutions, respectively. Each solution was placed in a glass vial, whose top incorporated a rubber septum. Standardized $^{99}TcO_4^-$ (0.28 M) was added in a slight molar excess (50 μL for 50 mg of POM, 90 μL for 100 mg, 170 μL for 200 mg, and 340 μL for 400 mg). The vials were then sealed, and the solutions purged with N_2 for 30 min before placing on a windowsill. These samples were exposed to sunlight over a period of 2 months. The solutions were monitored via ^{31}P NMR, UV−vis spectroscopy, and radio TLC. The 4 mM solution was also examined by EXAFS and XANES.

Preparation of UV−vis Spectroscopy Samples. UV−vis data were collected on samples prepared by the previous three methods outlined above. Samples of different starting concentrations (4−32 mM) were diluted by transferring 10, 5, 2.5, and 1.25 μL of each solution, respectively, to a quartz cuvette containing 1 mL of the appropriate reduction solution to yield same concentrations. Collected spectra were constricted between 400−800 nm to avoid saturation due to the large O−W ligand-to-metal charge transfer (LMCT) band in the 200−400 nm region.

EXAFS Spectroscopy. Two samples, a standard of chemically synthesized **$^{99}Tc^{V}$O-α2**[40] and a sample generated by in situ reduction using sunlight (4 mM of **α2**) were transferred to 2 mL screw capped, polypropylene centrifuge tubes, which were sealed inside two, nested polyethylene bags. Data were acquired at room temperature in transmission using Ar-filled ion chambers and in fluorescence using a 32 element Ge detector at SSRL beamlines 11−; data were collected using the locally written program XAScollect. Harmonic content of the beam was reduced by detuning the monochromator by 50%. Fluorescence data were corrected for detector deadtime, which was determined by adjusting the deadtime for each channel until the fluorescence XANES spectrum matched the transmission XANES spectrum. The data were processed using EXAFSPAK and Athena/ifeffit.[52,53] Data were fit using Artemis/ifeffit and theoretical phases and amplitudes calculated using FEFF7.[54] The initial model used in the FEFF calculation was $(NH_4)_6(P_2W_{18}O_{62})$ with one W atom replaced by ^{99}Tc.[55] Additional scattering shells were added only if their inclusion lowered the value of reduced χ^2. XANES spectra were fit using the locally written code "fites."

The F-test was used to analyze the significance of the fitting parameters, including the significance of adding a scattering shell.[56] The null hypothesis is that the additional shell of atoms does not improve the fit. The result of the F-test is the probability, p, that this hypothesis is correct. If $p < 0.05$, the null hypothesis is rejected in favor of the alternative hypothesis that the additional shell significantly improves the fit.[57]

RESULTS AND DISCUSSION

In-situ Reduction of MO_4^- (M = ^{99}Tc, Re) by K_{10}(α2-$P_2W_{17}O_{61}$) (α2) via UV Irradiation. There is momentum in the scientific community to employ "green" strategies for photocatalytic reduction of organic materials and metal ions to metallic nanoparticles using plenary POMs.[17−19,23,25,26,30,35,37,58−65] These plenary POMs can be reduced by multiple electrons while maintaining their structural integrity and acting as cathodes to efficiently transfer electrons to the organic material or metal. The reoxidized plenary ion thus stabilizes the reduced organic material or metal nanoparticle by electrostatic surface interactions.[17−19,37−39,63,64] We have found that the plenary Keggin ions $(PW_{12}O_{40})^{3-}$, $(SiW_{12}O_{40})^{4-}$, and $(AlW_{12}O_{40})^{5-}$ photocatalytically reduce $^{99}TcO_4^-$ to low-valent ^{99}Tc ($^{99}Tc^{V}$) and stabilize it.[66]

Here we employ photoactivation of the lacunary **α2** for reduction of $^{99}TcO_4^-$ and ReO_4^- and the complexation of the reduced metal into the defect binding site. The **α2** accepts electrons from a sacrificial electron donor and transfers these electrons to $^{99}TcO_4^-$ for reduction to $^{99}Tc^{V}$ quantitatively in a "one-pot" reaction. Moreover, the reoxidized **α2** can quantitatively incorporate the generated $^{99}Tc^{V}$ and Re^{V} covalently into the framework via bonding to the four basic oxygen atoms that comprise the **α2** defect site. This covalent bonding may be stronger compared to stabilization via electrostatic interactions, as described for the plenary POMs. This study serves as a

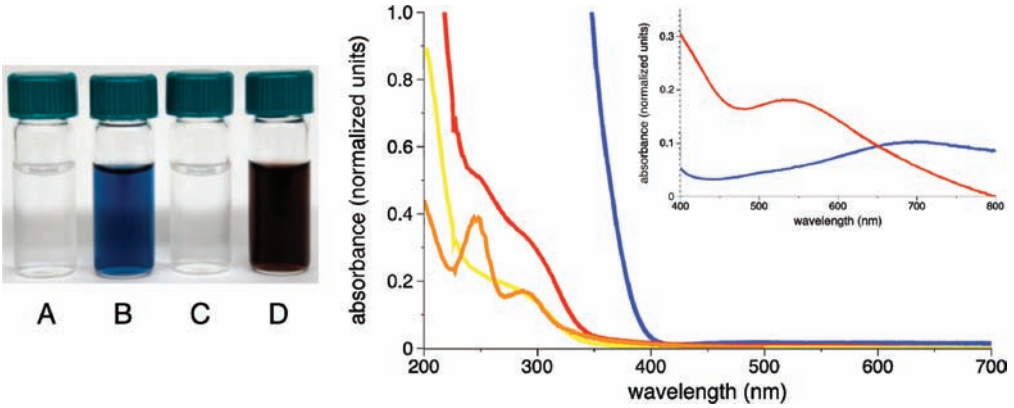

Figure 3. Color changes and UV−vis absorbances obtained during the photolytic reduction of $^{99}TcO_4^-$ using α_2-$[P_2W_{17}O_{61}]^{10-}$. Upon exposure to sunlight in the presence of 2-propanol, the clear colorless α_2-$[P_2W_{17}O_{61}]^{10-}$ (A, yellow trace) becomes reduced and exhibits the characteristic blue solution (B, blue trace). Upon addition of a clear colorless solution of $^{99}TcO_4^-$ (C, orange trace), the solution changes color from blue to dark orange (D, red trace). The inset is a 10× magnification of the 400−800 nm region.

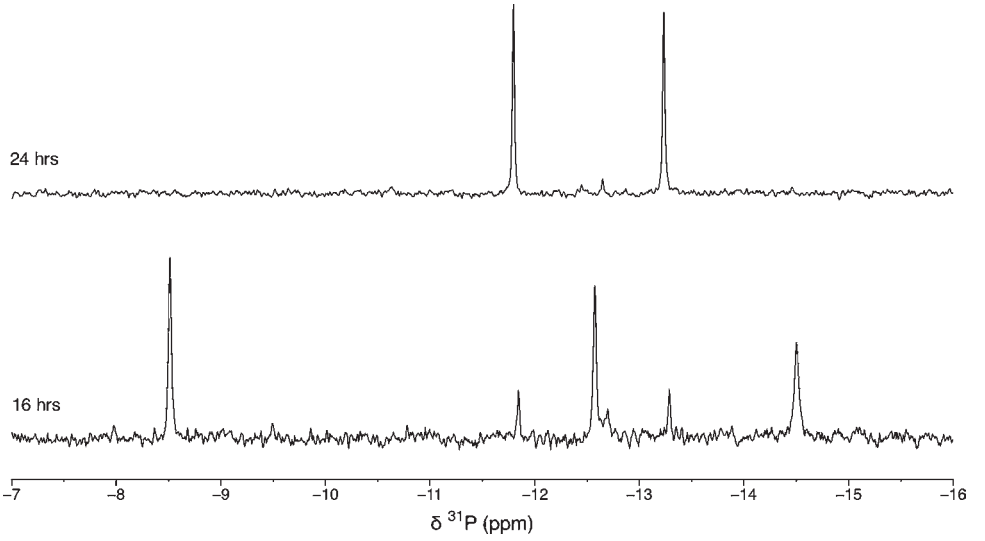

Figure 4. ^{31}P NMR for irradiation of $^{99}TcO_4^-$ in the presence of α_2-$[P_2W_{17}O_{61}]^{10-}$ and 2-propanol, D_2O, and 0.5 M of H_2SO_4 (1:1:2 vol). Concentrations of α_2-$[P_2W_{17}O_{61}]^{10-}$ are 4 mM (Table 1 shows chemical shift and integration data).

prototype to potential "green" strategies that may be used to reduce $^{99}TcO_4^-$ in the environment and sequester the reduced ^{99}Tc.

Reduction of $^{99}TcO_4^-$ and Formation of $^{99}Tc^{V}O(\alpha_2$-$P_2W_{17}O_{61})^{7-}$ ($^{99}Tc^{V}O$-α2). "One-pot" irradiation reactions were examined at concentrations of 4, 8, and 16 mM of ***α*2** in the presence of 1.2 mol equiv of $^{99}TcO_4^-$ under acidic conditions with and without electrolyte. The slight excess of ^{99}Tc was important to ensure that ^{31}P NMR could monitor the process conveniently. The ^{99}Tc speciation was monitored by radio TLC (monitoring the β^- of ^{99}Tc), and ^{99}Tc NMR gives an excellent handle for the $^{99}TcO_4^-$. The inclusion of 0.5 M of Na_2SO_4 as an electrolyte in the UV irradiation experiments was found to expedite the kinetics of the reactions.

While the UV irradiation reactions discussed below were performed as "one pot" reactions for ^{31}P NMR and radio TLC data, the reactions can be performed in stages provided that they are relatively airtight. The stepwise reactions shown in Figure 3 demonstrate the distinct color and UV−vis spectral changes. Upon reduction, the ***α*2** turns blue in color (λ_{max} = 700 nm) due to the mixed valent reduced species. Upon addition of clear, colorless $^{99}TcO_4^-$, the solution takes on the red-brown (λ_{max} = 540 nm) color of the $^{99}Tc^{V}O$-***α*2** complex.

The "one-pot" UV irradiation solutions, in the absence of electrolyte, showed a visible color change from clear and colorless to light orange-brown after 16 h of irradiation. This is consistent with the reduction of $^{99}Tc^{VII}$ and incorporation of $^{99}Tc^{V}$ into the ***α*2** framework. After 24 h, the more intensely colored orange-brown solutions suggest an increased concentration of $^{99}Tc^{V}O$-***α*2**. Figure S3, Supporting Information, shows the control experiment wherein $^{99}TcO_4^-$ is irradiated in the identical reduction solution but without the POM, demonstrating no change in the UV−vis spectrum.

The reaction mixtures at all concentrations, 4, 8, and 16 mM, were monitored by ^{31}P NMR spectroscopy during irradiation at 16 and 24 h (Figure 4 (4 mM) and Figure S4 (8 and 16 mM), Supporting Information). The irradiation was ceased at 24 h, and the 8 and 16 mM solutions were monitored for a further 72 h

Table 1. Multinuclear ^{31}P NMR Data for Irradiation of $^{99}TcO_4^-$ and ReO_4^- in the Presence of α_2-$[P_2W_{17}O_{61}]^{10-}$ and 2-Propanol at Concentration of 4 mM of α2-$[P_2W_{17}O_{61}]^{10-}$ at 25°C As a Function of Time[a]

	^{31}P NMR (ppm, integrations reported as % of whole spectrum)								
time of irradiation at 254 nm	δ, ppm M^VO-**α2** (M = ^{99}Tc,Re)	integral	δ, ppm **α2** ligand	integral	δ, ppm intermediate	integral	δ, ppm $P_2W_{18}O_{62}$	integral
	4 mM Solution (1:1.2 α2-$[P_2W_{17}O_{61}]^{10-}$:$^{99}TcO_4^-$ without Added Na_2SO_4)							
16 h	−11.84, −13.29	9.06	−8.51, −12.58	61.3	−14.50	23.16	−12.70	6.47
24 h	−11.79, −13.24	94.07	−12.45	3.19	–	–	−12.68	2.77
	4 mM Solution (1:1.2 α2-$[P_2W_{17}O_{61}]^{10-}$:$^{99}TcO_4^-$ Containing Na_2SO_4)							
16 h	−11.84, −13.29	33.00	−12.58	18.88	−14.50	48.00	–	–
24 h	−11.79, −13.29	57.11	–	–	−14.45	42.88	–	–
72 h p.i.	−11.79, −13.29	100	–	–	–	–	–	–
	4 mM Solution (1:1 α2-$[P_2W_{17}O_{61}]^{10-}$:$^{99}TcO_4^-$ Containing Na_2SO_4)							
16 h		0	−8.22, −12.51	59	−14.19	41	–	–
5 h p.i.	−11.67, −13.22	8	−8.30, −12.59	60	−14.28	32	–	–
19 h p.i.	−11.76, −13.32	18	−8.38, −12.66	57	−14.38	25	–	–
24 h p.i.	−11.75, −13.30	28	−8.37, −12.65	40	−14.37	31	–	–
	δ, ppm Re^VO-**α2**	integral	δ, ppm **α2** ligand	integral	δ, ppm intermediate	integral	δ, ppm $P_2W_{18}O_{62}$	integral
	4 mM Solution (1:1.2 α2-$[P_2W_{17}O_{61}]^{10-}$:ReO_4^- Containing Na_2SO_4)							
16 h	−12.21, −13.21	100	–	–	–	–	–	–

[a] These samples possess stoichiometry of 1:1.2 α2-$[P_2W_{17}O_{61}]^{10-}$: $^{99}TcO_4^-$ or ReO_4^- and 1:1 α2-$[P_2W_{17}O_{61}]^{10-}$: $^{99}TcO_4^-$, as indicated in the table. All cases except one, as indicated, contain 0.5M of Na_2SO_4. The ^{31}P NMR spectra corresponding to these samples are shown in Figures 4−6 for ^{99}Tc and Figure 7 for Re. The integrations are reported as % of the entire spectrum.

after the irradiation was stopped (Figure S4, Supporting Information). Table 1 and Table S1, Supporting Information, identify the species and the relative integrations for 4, 8, and 16 mM concentrations, respectively. The species formed in this series of reactions as well as in those with electrolyte (vide infra) are: (1) **$^{99}Tc^VO$-α2** (−11.84 and −13.29 ppm); (2) an "intermediate" that subsequent studies suggest contains ^{99}Tc and phosphorus (−14.50 ppm); (3) unreacted **α2** (−8.51 and −12.58 ppm); and (4) the decomposition product, α-$[P_2W_{18}O_{62}]^{6-}$ (−12.65 ppm). These chemical shifts (except for the ^{99}Tc/P containing intermediate) have been assigned previously in independent studies where **$^{99}Tc^VO$-α2** has been chemically synthesized and characterized.[40]

The ^{31}P NMR of the 4 mM **α2** reaction (Figure 4) is straightforward and exemplifies the reaction speciation: after 16 h of irradiation the ^{31}P NMR shows significant amounts of "free" **α2** ligand (60% integrated intensity of entire spectrum), modest amounts of **$^{99}Tc^VO$-α2** (9%), and an appreciable quantity of the ^{99}Tc/P-containing intermediate (−14.50 ppm, 23%). While complexes of **α2** require that the two inequivalent P atoms show two resonances, we postulate that the intermediate contains a paramagnetic center, since only one resonance is observed for the intermediate in this media. XANES data collected on a sample containing the intermediate (discussed later) are consistent with a ^{99}Tc(IV)-containing species. The paramagnetic center would likely result in broadening of the resonance of the P atom close to the site of substitution. All ^{31}P NMR integration data reported here are based on 100% of the resonances observed. While comparisons of integration of the ^{31}P NMR spectra cannot give quantitative data, trends in the amounts of intermediate compared to **$^{99}Tc^VO$-α2** and **α2** ligand with irradiation, concentration, and time can be determined.

As the reaction progresses, the resonances due to the **α2** ligand and the intermediate species decrease, while those for **$^{99}Tc^VO$-α2** increase (>90%) (Figure 4). After 24 h of irradiation **$^{99}Tc^VO$-α2** (>90%) is formed predominantly, accompanied by trace amounts of the decomposition product, α-$[P_2W_{18}O_{62}]^{6-}$ (−12.65 ppm). No ^{99}Tc/P-containing intermediate is observed after 24 h. This ^{31}P NMR speciation study suggests that during the irradiation **α2** is reduced. The reduced **α2** in turn transfers electrons to $^{99}TcO_4^-$ to form **$^{99}Tc^VO$-α2** and/or the ^{99}Tc/P-containing intermediate species, which then converts to **$^{99}Tc^VO$-α2**.

Comparison of the ^{31}P NMR spectra for the 4 mM with 8 and 16 mM samples (Figure 4 and Table 1 and Figure S4 and Table S1, Supporting Information) at 16 h of irradiation clearly shows the concentration dependence of the ^{99}Tc/P-containing intermediate compared to the **$^{99}Tc^VO$-α2**. The intermediate decreases at high concentrations compared to the **$^{99}Tc^VO$-α2**; little or no intermediate is observed at 16 mM (Figure S4, Supporting Information). In the 8 mM sample (Figure S4, Supporting Information), the intermediate is converted to the **$^{99}Tc^VO$-α2** during the 72 h period of no irradiation. The decomposition product, α-$[P_2W_{18}O_{62}]^{6-}$ (−12.65 ppm), is observed in the 8 mM and is more prevalent in the 16 mM sample. These spectra show a very broad resonance at −8.51 ppm (assigned to the **α2** ligand) that is attributed to the two electron-reduced α_2-$[P_2W_{17}O_{61}]^{12-}$ participating in electronic exchange with the oxidized **α2**. This phenomenon has been observed in systems containing high concentrations of α-$[P_2W_{18}O_{62}]^{6-}$.[67]

Irradiation of the solutions containing 0.5 M Na_2SO_4 suggests that the electrolyte facilitates the electron-transfer reactions (Figure S5, Supporting Information). At all concentrations an increase in the ^{99}Tc/P-containing intermediate, compared to solutions that do not contain electrolyte, was observed. Moreover, the

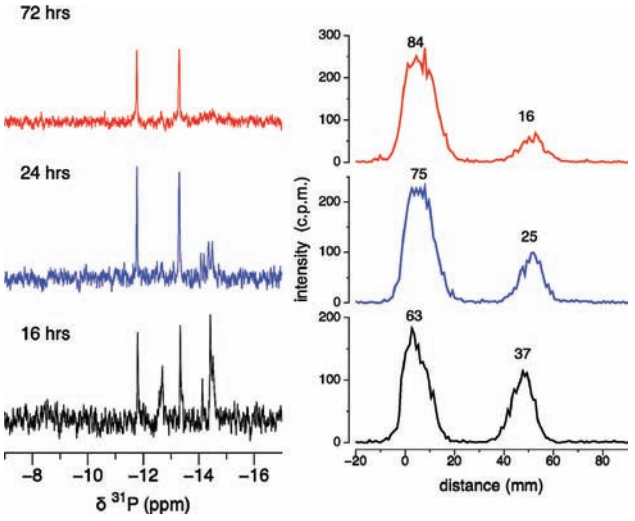

Figure 5. Radio TLC chromatograms (monitoring β emission of ^{99}Tc) for UV irradiation of $^{99}TcO_4^-$ in the presence of α_2-$[P_2W_{17}O_{61}]^{10-}$. $^{99}Tc^VO(\alpha_2\text{-}P_2W_{17}O_{61})^{7-}$ and ^{99}Tc/P containing intermediate remain at the origin; $^{99}TcO_4^-$ moves with the solvent front. The reduction solvent was a mixture of 2-propanol, D_2O, and 0.5 M H_2SO_4 (containing 0.5 M Na_2SO_4) (1:1:2 vol). The concentration of α_2-$[P_2W_{17}O_{61}]^{10-}$ is 4 mM. Irradiation times are 16 and 24 h. Also shown is the time point at 72 h after cessation of irradiation. The numbers above the TLC peaks are the relative integrations of the radioactivity. Shown on the left side of the figure are the ^{31}P NMR spectra for the same samples.

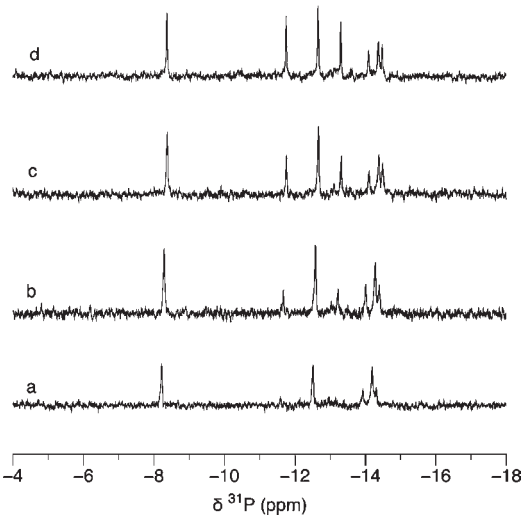

Figure 6. ^{31}P NMR for irradiation of $^{99}TcO_4^-$ in the presence of α_2-$[P_2W_{17}O_{61}]^{10-}$ with 1:1 POM:$^{99}TcO_4^-$ stoichiometry. The reduction solvent is a mixture of 2-propanol, D_2O, and 0.5 M H_2SO_4 containing 0.5 M Na_2SO_4 supporting electrolyte (1:1:2 vol). The concentration of α_2-$[P_2W_{17}O_{61}]^{10-}$ is 4 mM. Irradiation is stopped after 19 h (a), and the ^{31}P NMR is observed 5 (b), 19 (c), and 24 h (d) after cessation of irradiation.

intermediate persists in solution (Figure S5 and Table S2, Supporting Information) and is concentration dependent. At 4 mM, with Na_2SO_4 electrolyte present, the intermediate consists of three peaks. This suggests that, in the media-containing Na_2SO_4 electrolyte, at least two intermediate species exist. For all concentrations, the intermediate species converts to **$^{99}Tc^VO$-α2** during the 72 h post irradiation. The decomposition product α-$[P_2W_{18}O_{62}]^{6-}$ is observed for 8 and 16 mM concentrations. The amount of α-$[P_2W_{18}O_{62}]^{6-}$ decomposition product formed at higher concentrations is expected from the stability studies described in the Supporting Information (Figure S2).

The combination of the radio TLC and the ^{31}P NMR data shows the progression of the reactions and provides evidence that the intermediate is composed of ^{99}Tc as well as ***α*2** POM. While the integrated intensities in the ^{31}P NMR are qualitative (in terms of absolute concentrations), the observed trends in the NMR track very well with the radio TLC data. For example, Figure 5 shows the radio TLC data along with the ^{31}P NMR data for the 4 mM sample. In the TLC experiment, POMs, **$^{99}Tc^VO$-*α*2** and the ^{99}Tc/P-containing intermediate, remain at the origin, and $^{99}TcO_4^-$ moves with the solvent front. At 16 h, 63% of the activity remains at the origin, and 37% of the activity moves with the solvent front. The integrated intensities of the ^{31}P NMR (Table 1) shows 81% ^{99}Tc POM species (33% **$^{99}Tc^VO$-*α*2** + 48% ^{99}Tc/P-containing intermediate). Correcting for the excess $^{99}TcO_4^-$ in the experiment, the calculated percentages, 67.5% activity as ^{99}Tc POM species (that would remain at the origin) and 32.5% activity as $^{99}TcO_4^-$ (that would move with the solvent front), are in good agreement with the observed radio TLC data. In addition to radio TLC and ^{31}P NMR, ^{99}Tc NMR shows that the excess ^{99}Tc remains as $^{99}TcO_4^-$. See Supporting Information for details. This is further confirmed in the EXAFS/XANES experiments (vide infra).

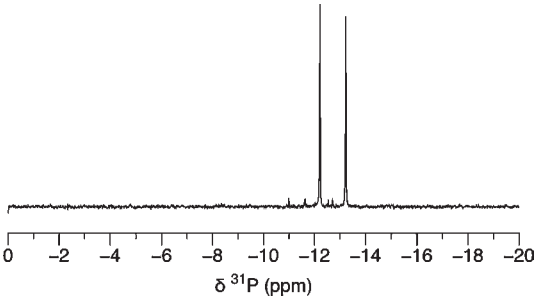

Figure 7. ^{31}P NMR for irradiation of ReO_4^- in the presence of 4 mM α_2-$[P_2W_{17}O_{61}]^{10-}$ at 16 h. The solvent was a mixture of 2-propanol, D_2O, and 0.5 M H_2SO_4 (containing 0.5 M Na_2SO_4) (1:1:2 vol). The concentrations 8 and 16 mM are shown in Figure S7, Supporting Information.

Irradiation of 4 mM ***α*2** in solutions comprised of 1:1 ***α*2**:$^{99}TcO_4^-$ stoichiometry with 0.5 M Na_2SO_4 electrolyte for 19 h resulted exclusively in the intermediate species and ***α*2** (Figure 6 and Table 1). The three resonances that comprise the intermediate species in the electrolyte solution are quite pronounced at this stoichiometry. The solution was monitored by ^{31}P NMR after irradiation was ceased. As observed for the cases above wherein a slight excess of $^{99}TcO_4^-$ was maintained, the intermediate is seen to convert to product over time.

The addition of KCl under airtight conditions, followed by cooling of the solution resulted in a crystalline solid. ^{31}P NMR of the solid redissolved in D_2O shows the intermediate species and ***α*2**, confirming that isolation does not compromise the integrity of the intermediate. While the nature of the intermediate needs to be further evaluated, the X-ray absorption spectroscopy (XAS) studies, described below, suggest that the intermediate may be comprised of a partially coordinated ^{99}Tc(IV) species.

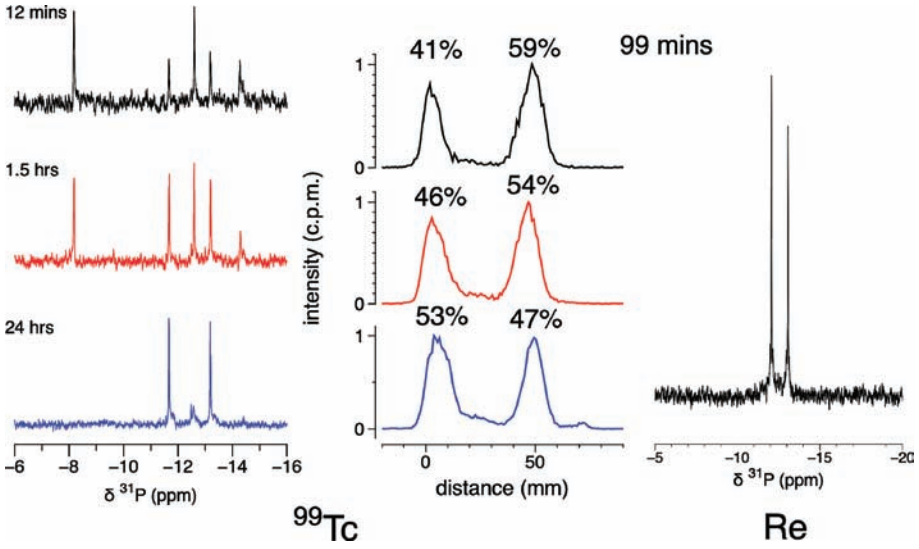

Figure 8. Comparison of reductions of $^{99}TcO_4^-$ and ReO_4^- by reduced $\alpha 2$-$[P_2W_{17}O_{61}]^{12-}$ (produced by bulk electrolysis): Solutions for both experiments consist of 5 mM α_2-$[P_2W_{17}O_{61}]^{10-}$ in a 0.5 M H_2SO_4 (containing 0.5 M Na_2SO_4):D_2O mixture (1:1 vol, 20 mL). ^{31}P NMR spectra (left, 25 °C, D_2O) and radio TLC (center) for ^{99}Tc at 12 min and 1.5 and 24 h after addition of $^{99}TcO_4^-$ to reduced α_2-$[P_2W_{17}O_{61}]^{12-}$. ^{31}P NMR spectrum for Re (right) at 99 min after addition of ReO_4^- to reduced α_2-$[P_2W_{17}O_{61}]^{12-}$. Two resonances at −12.20 and −13.20 ppm represent product $Re^VO(\alpha_2$-$P_2W_{17}O_{61})^{7-}$ and match the chemically synthesized $Re^VO(\alpha_2$-$P_2W_{17}O_{61})^{7-}$. Note at the same time point (1.5 h), the ^{99}Tc sample shows 42% product as well as α_2-$[P_2W_{17}O_{61}]^{10-}$ and the ^{99}Tc/P-containing intermediate.

Reduction of ReO_4^- and Formation of $Re^VO(\alpha_2$-$P_2W_{17}O_{61})^{7-}$ (Re^VO-$\alpha 2$). Irradiation (at 254 nm) of a solution consisting of $\alpha 2$ in the reduction solution containing 0.5 M Na_2SO_4 and ReO_4^- results in the formation of Re^VO-$\alpha 2$. This parallels the previous experiments with $^{99}TcO_4^-$. The ^{31}P NMR data are presented in Figure 7 (4 mM $\alpha 2$) and Figure S6, Supporting Information, (8 mM and 16 mM $\alpha 2$) and summarized in Table 1 and Table S3, Supporting Information. All three concentrations of $\alpha 2$ were irradiated under the same conditions for 16 h. For the lowest concentration, 4 mM, formation of >99% of the Re^VO-$\alpha 2$ product is complete after 16 h of irradiation. Significant amounts of free $\alpha 2$ ligand are observed to remain in solution for the 8 and 16 mM samples. This is to be expected as all samples were exposed to the same intensity light source for an equal amount of time.

To monitor the radio TLC, a 4 mM reaction was "spiked" with ^{188}Re, a radioactive tracer. After irradiation for 16 h with 254 nm light, the ^{31}P NMR (Figure S7, Supporting Information) shows a predominance of the Re^VO-$\alpha 2$ complex. The speciation, assessed by radio TLC developed in saline (Figure S7, Supporting Information) shows that 75% of activity remains at the origin ($^{188}Re^VO$-$\alpha 2$). The 25% excess activity that migrates with the solvent front is due to the excess $^{188}ReO_4^-$ in the irradiation reaction. This behavior is consistent with the ^{31}P NMR showing >99% Re^VO-$\alpha 2$ product formation.

The reduction of ReO_4^- and incorporation of the reduced Re into the $\alpha 2$ framework at all concentrations is significantly faster than for the ^{99}Tc analogs (NMR data for corresponding ^{99}Tc reactions are shown in Figure 5 and Table 1 and Figure S5 and Table S2, Supporting Information). Formation of the Re^VO-$\alpha 2$ complex at 4 mM was complete in 16 h, while the analogous ^{99}Tc reaction showed 33% $^{99}Tc^VO$-$\alpha 2$, approximately 48% of the ^{99}Tc/P-containing intermediate and 19% $\alpha 2$ ligand at 16 h. This observation appears inconsistent with ^{99}Tc/Re periodic trends where the reduction of rhenium compared to technetium in acidic aqueous solution is consistently more difficult (by ~120 mV) and the kinetics are slower.[41,42,68,69] However, we observe no formation of an intermediate species in any reactions with Re. It is likely that the mechanisms of the ^{99}Tc and Re reactions differ.

Reduction of MO_4^- (M = ^{99}Tc, Re) by $\alpha 2$-$[P_2W_{17}O_{61}]^{12-}$ Generated by Bulk Electrolysis. To further probe the reduction and incorporation of M^VO (M = ^{99}Tc, Re) into the $\alpha 2$ framework, we employed bulk electrolysis to completely reduce the $\alpha 2$ ligand by two electrons prior to addition of MO_4^-.

$^{99}TcO_4^-$. The reduced α_2-$[P_2W_{17}O_{61}]^{12-}$ was produced by bulk electrolysis by applying a voltage of −220 mV to a 5 mM solution of $\alpha 2$ dissolved in 1:1 0.5 H_2SO_4 (containing 0.5 M Na_2SO_4):D_2O via the working electrode. The characteristic blue color of reduced POM appeared immediately. Under inert atmosphere, the rest potential of the reduced POM solution remained constant over a period of 30 min, thus ensuring that the α_2-$[P_2W_{17}O_{61}]^{12-}$ remained reduced once the applied potential was removed. Upon addition of degassed $^{99}TcO_4^-$ (1.4 equiv) to the blue solution, under gentle stirring, the rest potential began to increase to more positive potential, and the solution slowly changed from a dark blue to a dark red-brown color.

The rest potential initially increased from −220 to −85 mV over the first 30 s (Figure S8A, Supporting Information), indicating that the α_2-$[P_2W_{17}O_{61}]^{12-}$ oxidized to $\alpha 2$ coupled to a reduction of $^{99}TcO_4^-$. The rate of the change slowed down between 30 s and 5 min then increased rapidly to reach another plateau after 21 min. From 21 min up to 48 h, the rest potential very slowly increased to +393 mV. The sharp jump of +135 mV in the first 30 s and the consequent plateau after 5 min after addition of $^{99}TcO_4^-$ supports the hypothesis that α_2-$[P_2W_{17}O_{61}]^{12-}$ is rapidly transferring electrons to $^{99}TcO_4^-$, and the slow rise in rest potential suggests that a reduced form of ^{99}Tc is slowly incorporating into the POM framework. ^{31}P NMR and radio TLC were used to monitor the course of the reaction.

^{31}P NMR data, collected 12 min and 1.5 h and 24 h post $^{99}TcO_4^-$ addition (Figure 8 and Table S4, Supporting Information) show the same speciation as for the photoactivated

Scheme 1. Possible Mechanisms for the Reduction of MO_4^- (M = ^{99}Tc, Re) and Incorporation of Reduced M into α_2-$[P_2W_{17}O_{61}]^{10-}$ [a,b]

^{99}Tc:

α_2-$[P_2W_{17}O_{61}]^{10-}$ + 2 e^-	→	α_2-$[P_2W_{17}O_{61}]^{12-}$	step 1
α_2-$[P_2W_{17}O_{61}]^{12-}$ + $^{99}Tc^{VII}O_4^-$	→	^{99}Tc /P containing intermediate [a]	step 2 Fast
^{99}Tc/P containing intermediate	→	$^{99}Tc^{V}O(\alpha_2$-$P_2W_{17}O_{61})^{7-}$	step 3 Slow RDS

Re:

α_2-$[P_2W_{17}O_{61}]^{10-}$ + 2 e^-	→	α_2-$[P_2W_{17}O_{61}]^{12-}$	step 1
α_2-$[P_2W_{17}O_{61}]^{12-}$ + $Re^{VII}O_4^-$	→	$Re^{VII}O_4^-$: α_2-$[P_2W_{17}O_{61}]^{12-}$ [b]	step 2 Fast
$Re^{VII}O_4^-$: α_2-$[P_2W_{17}O_{61}]^{12-}$	→	$Re^{V}O(\alpha_2$-$P_2W_{17}O_{61})^{7-}$	step 3 Slow RDS

[a] The ^{99}Tc containing intermediate is observed in the ^{31}P NMR and XAS experiments suggest that this is a ^{99}Tc(IV) α2 species. [b] While the Re reactions do not show an intermediate, expansion of the ReO_4^- coordination sphere may result in a ReO_4^-:***α*2** complex that facilitates reduction. See text for complete descriptions. The designation of "slow" denotes the rate-limiting step (RDS) and does not reflect the speed of the reaction.

reduction experiments: free ***α*2**, the **^{99}Tc^{V}O-*α*2** complex, the ^{99}Tc/P-containing intermediate, and the plenary α-$[P_2W_{18}O_{62}]^{6-}$ decomposition product. The speciation observed in the ^{31}P NMR data correlates with the observed rest potential changes as a function of time.

The combination of ^{31}P NMR spectroscopy and rest potential over the course of the reaction suggests a mechanism wherein the reduction of $^{99}TcO_4^-$ is rapid, and initially a ^{99}Tc/P-containing intermediate is formed. This is indicated by the combination of the initial rise in rest potential (after 30 s) and plateau at 5 min and the ^{31}P NMR, after 12 min, showing the formation of the intermediate species. The conversion of that intermediate species to **^{99}Tc^{V}O-*α*2** is consistent with the second increase in the rest potential to a plateau after 21 min. This correlates to the ^{31}P NMR after 1.5 h showing a significant increase in the **^{99}Tc^{V}O-*α*2** and a decrease in the ^{99}Tc-intermediate. The observation of the ***α*2** lacunary in the ^{31}P NMR after 1.5 h, coupled with the >80% **^{99}Tc^{V}O-*α*2** formation at 24 h, attests to the slow incorporation of reduced ^{99}Tc into the ***α*2** lacunary site.

Radio TLC performed on the reaction solution at the same time points as for the ^{31}P NMR (Figure 8) track the ^{31}P NMR data, further suggesting that the intermediate species contains ^{99}Tc and P and is likely a ^{99}Tc-***α*2** containing species (see Supporting Information). The intermediate undergoes a slow conversion to a **^{99}Tc^{V}O-*α*2** product.

Figure S9A, Supporting Information, shows the CV of ***α*2** before and after bulk electrolysis and 48 h after the addition of TcO_4^-. It can be seen that after 48 h a new redox wave appears ca. 800 mV. This is attributed to the **^{99}Tc^{V}O-*α*2** species where the $^{99}Tc^{V}$ is incorporated into the POM framework. The CV is identical to the chemically synthesized **K-^{99}Tc^{V}O-*α*2** complex[40] (Figure S9A, Supporting Information). The symmetrical peak at ca. 630 mV is a stripping wave of the $^{99}TcO_4^-$ from the working GC electrode. This wave is visible only when scans are made to potentials lower than −550 mV and indicates, as expected, the presence of excess $^{99}TcO_4^-$.

ReO_4^-. The production of reduced α_2-$[P_2W_{17}O_{61}]^{12-}$ (by bulk electrolysis) and subsequent reduction of ReO_4^- was conducted under the same conditions at the ^{99}Tc experiment. As described below, the two metals behave differently. Upon addition of the degassed ReO_4^- solution to the reduced α_2-$[P_2W_{17}O_{61}]^{12-}$ solution, the rest potential increased (Figure S8B, Supporting Information), and the solution quickly changed from a dark blue to a purple color. The rest potential increased from −220 to −104 mV after 30 s, which indicates that the α_2-$[P_2W_{17}O_{61}]^{12-}$ is being oxidized to ***α*2** in conjunction with the reduction of ReO_4^-. The rate of the change in reduction potential then slows down and plateaus after 60 min at around 26 mV. There is only one plateau in the rest potential change for the Re experiment compared to the ^{99}Tc experiment, where there were two plateaus.

The ^{31}P spectrum of the solution (Figure 8), taken 1.5 h after the addition of ReO_4^-, shows exclusively **Re^{V}O-*α*2** product; the spectrum is identical to that of chemically synthesized **Re^{V}O-*α*2**.[46] An intermediate species is never observed in the ^{31}P NMR for any of the Re experiments. At the same time point (1.5 h), the ^{99}Tc analog showed 42% **^{99}Tc^{V}O-*α*2** product, 11% intermediate, and 47% ***α*2**. Reduction of ReO_4^- and incorporation of reduced rhenium into the ***α*2** framework is faster than that of ^{99}Tc, and as no intermediate is observed in the Re reactions, it is likely that the Re reactions occur by a different mechanism than that of ^{99}Tc. This set of experiments demonstrates a significant difference between technetium and rhenium.

Figure S9B, Supporting Information, shows the CV of ***α*2** before and after bulk electrolysis and 99 min after the addition of ReO_4^-. It can be seen that after 99 min a new redox wave appears ca. 260 mV, which is due to an incorporated Re species into the POM framework. The CV is identical to the chemically synthesized **K-Re^{V}O-*α*2** complex[40]

This experiment supports a rapid reduction of both rhenium (VII) and technetium (VII) as evidenced by the rapid rise in the rest potential upon addition of MO_4^- to the reduced α_2-$[P_2W_{17}O_{61}]^{12-}$. After this initial rapid rise in rest potential, ^{99}Tc and Re differ. The ^{99}Tc undergoes a slow rise in rest potential to form a plateau after 21 min and then another plateau after approximately 48 h. This timing tracks with the observation of the ^{99}Tc/P intermediate in the NMR and TLC and the slow conversion of the intermediate into the **^{99}Tc^{V}O-*α*2** product. Alternatively, the Re reaches a single final plateau after 60 min tracking with the NMR data that shows complete conversion to the **Re^{V}O-*α*2** product in 1.5 h.

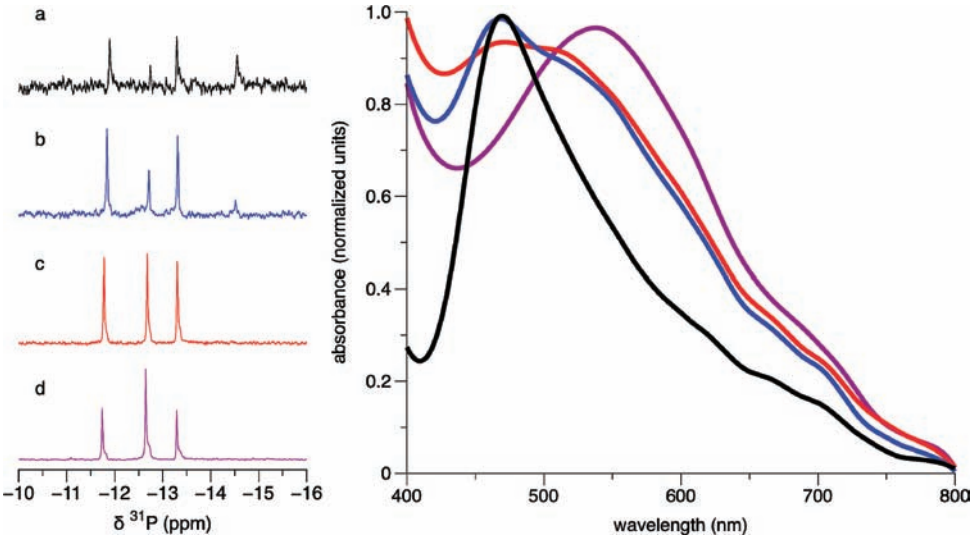

Figure 9. ^{31}P NMR (left) and normalized UV−vis spectra (right) of $^{99}TcO_4^-$ and α_2-$[P_2W_{17}O_{61}]^{10-}$ in 0.5 M of H_2SO_4, D_2O, and 2-propanol (2:1:1 vol) following exposure to sunlight for 2 months as a function of concentration. (a) 4 mM (black traces); (b) 8 mM (blue traces); (c) 16 mM (orange traces); and (d) 32 mM (red traces). The minor absorbances between 650 and 800 nm are due to trace amounts of reduced α-$[P_2W_{18}O_{62}]^{6-}$.

Comparison of the Two Approaches. The interaction of $^{99}TcO_4^-$ and ReO_4^- with reduced α_2-$[P_2W_{17}O_{61}]^{12-}$, formed by photoactivation/reduction of ***α*2** in the presence of 2-propanol, and with reduced α2-$[P_2W_{17}O_{61}]^{12-}$, that is generated by bulk electrolysis, shows identical products according to ^{31}P NMR and consistent kinetic profiles. For ^{99}Tc, these products include **$^{99}Tc^{V}O$-*α*2** and the ^{99}Tc/P-containing intermediate. For Re, the **$Re^{V}O$-*α*2** product was observed with no intermediate. The kinetic trends are also the same: the ^{99}Tc reactions were always slower than the Re reactions. This may be due to a rapid reduction of both $^{99}TcO_4^-$ and ReO_4^- with a slow incorporation of the ^{99}Tc/P-containing intermediate to the **$^{99}Tc^{V}O$-*α*2** product and a relatively concerted mechanism for the formation of **$Re^{V}O$-*α*2**. The possibility of ReO_4^- for expansion of the coordination sphere to produce a ReO_4^-:***α*2** "complex" may facilitate a concerted incorporation/reduction step in the case of Re.[68,70,71] Potential mechanisms for both ^{99}Tc and Re are put forward in Scheme 1 (detailed discussion later).

The mechanism of the electron transport process from reduced α_2-$[P_2W_{17}O_{61}]^{12-}$ to $^{99}TcO_4^-$ likely differs in the two strategies. In the UV irradiation procedure, the ***α*2** ligand is continuously reduced upon irradiation in the presence of 2-propanol, and in turn, the reduced α_2-$[P_2W_{17}O_{61}]^{12-}$ continuously transfers electrons to $^{99}TcO_4^-$ to form the ^{99}Tc/P containing intermediate or into the **$^{99}Tc^{V}O$-*α*2** product. In contrast, the bulk electrolysis method generates reduced α_2-$[P_2W_{17}O_{61}]^{12-}$ all at once and will reduce a certain amount of $^{99}TcO_4^-$ before being consumed.

The UV−vis spectra for the **$^{99}Tc^{V}O$-*α*2** products formed by the two types of reactions along with the chemically synthesized **$^{99}Tc^{V}O$-*α*2** are compared in Figure S10, Supporting Information. The d−d band in the spectrum of the chemically synthesized product is identical to that produced by generating α_2-$[P_2W_{17}O_{61}]^{12-}$ via electrolysis (500 nm). The spectrum of the **$^{99}Tc^{V}O$-*α*2** product formed by the UV irradiation procedure shows an absorbance at 540 nm. While the ^{31}P NMR data are identical for the **$^{99}Tc^{V}O$-*α*2** products generated by the three methods, the UV-irradiated samples consistently show a red-shifted absorbance in the visible spectra.

The continued irradiation in an acidic mixture, containing 2-propanol, results in continuous reduction of the ***α*2** and concomitant oxidation of the 2-propanol. This process may result in a subtle but more complex ^{99}Tc speciation pattern than that for the procedure involving bulk electrolysis and that may underlie the UV−vis spectroscopic differences.[40,72] The persistence of a small amount of a ^{99}Tc(IV)-***α*2** species, such as the putative intermediate described below, may contribute to the sensitive visible spectra while not considerably impacting the ^{31}P NMR. Moreover, the degradation products of the 2-propanol or sulfate from the electrolyte may be ligating to the **$^{99}Tc^{V}O$-*α*2** product, also impacting the visible spectra but not necessarily the ^{31}P NMR or radio TLC. We plan to investigate this further in future studies.

Reduction of $^{99}TcO_4^-$ Using Photolytically Reduced K_{10}(α_2-$P_2W_{17}O_{61}$) (*α*2) in Sunlight. The most abundant source of light is sunlight, and the photoactivation of ***α*2** for reduction of $^{99}TcO_4^-$ and incorporation of the reduced ^{99}Tc does indeed occur with the sun as the source of irradiation. Although sunlight encompasses a continuum of wavelengths, not all wavelengths are efficient in photoexciting the POM. Moreover, the reduction samples were prepared in glass vials, which absorb much of the high-energy irradiation that would otherwise facilitate the reduction of ***α*2**. Not surprisingly, the reactions take longer than with a constant, controlled irradiation source.

Solutions of ***α*2** dissolved in the reduction solution and a 1.2 molar excess of $^{99}TcO_4^-$ were photolytically reduced using sunlight over a period of 2 months. The concentrations of POM in this experiment ranged from 4 to 32 mM. The formation of the dark-orange color provided evidence of $^{99}TcO_4^-$ reduction. The resulting solutions were monitored by UV−vis spectroscopy and ^{31}P NMR spectroscopy (Figure 9).

The ^{31}P NMR experiment reveals that, as observed for the UV photoactivated experiments, the ^{99}Tc/P-containing intermediate is more abundant at the lower concentrations. As expected, more α-$[P_2W_{18}O_{62}]^{6-}$ decomposition product (−12.66 ppm) is formed at the higher concentrations. In addition, the intermediate species appears more prevalent and longer lived when using sunlight for the photoactivation of the POM. Both the 4 and

8 mM concentration samples show a λ_{max} at 470 nm with a broad tail at the low-energy side. This can be explained by considering the ^{31}P NMR, where the **^{99}Tc^{V}O-α2** product and the intermediate are both observed. The highest concentration, 32 mM, shows a λ_{max} at 540 nm, identical to the absorbance observed for all of the photoactivated irradiations (Figure S10, Supporting Information); at this concentration no ^{99}Tc/P intermediate is observed in the ^{31}P NMR. The concentration of 16 mM shows a broad peak encompassing the two limiting wavelengths.

Clearly, sunlight may not be the most efficient light source for photocatalytic reduction of $^{99}TcO_4^-$ mediated by the **α2** POM. However, the above experiments provide proof of principal that this strategy works. Altering the POM to one that absorbs in the visible region,[73] sensitization of the POM using a transition metal[74] or employing a palette of POMs with a variety of absorbances may lead to a more efficient reduction of $^{99}TcO_4^-$ and incorporation of the reduced ^{99}Tc into the POM framework.

X-ray Absorption Fine Structure Spectroscopy Provides Information of ^{99}Tc/P Containing Intermediate. A solution of 4 mM **α2** dissolved in the reduction solution and a 1.2 molar excess of $^{99}TcO_4^-$ that was photolytically reduced using sunlight over a period of 2 months was subjected to EXAFS and XANES spectroscopy at the ^{99}Tc K-edge. The XANES spectrum of this sample is shown in Figure S11, Supporting Information, along with the XANES spectrum of **^{99}Tc^{V}O-α2**.[40] The half height of the absorption edge of intermediate spectrum is ~0.7 eV lower in energy than that of **^{99}Tc^{V}O-α2**, which is surprising in light of the fact that excess $^{99}TcO_4^-$ is present in this sample. Therefore, the spectrum of this sample was fit using the spectra of $^{99}TcO_4^-$, **^{99}Tc^{V}O-α2**[40], and ^{99}Tc(IV) gluconate (^{99}Tc(IV) gluconate is monomeric and has six oxygen neighbors at 2 Å) (see Figure S12 and Table S5, Supporting Information).[1] The XANES fit indicates that the sample consists of approximately 25% ^{99}Tc(VII), 55% ^{99}Tc(V), and 20% ^{99}Tc(IV). While the presence of ^{99}Tc(VII) in the sample is not unexpected (excess $^{99}TcO_4^-$ was present, and the reaction may not have proceeded to completion), the presence of ^{99}Tc(IV) suggests either that the intermediate is a ^{99}Tc(IV) species or that multiple intermediates (^{99}Tc(IV), ^{99}Tc(V)) exist. The presence of ^{99}Tc(IV) also explains the ^{31}P NMR spectrum in that the resonance of the P proximal to ^{99}Tc(IV) will be significantly shifted due to the local moment of the paramagnetic ^{99}Tc(IV) center and will also be strongly broadened by fast relaxation of the ^{31}P spin.

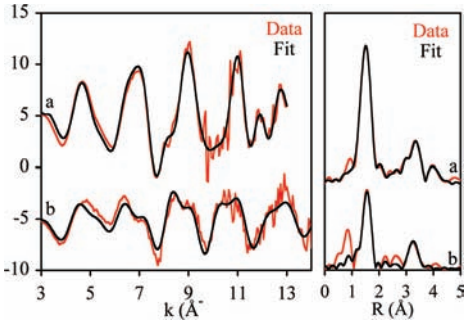

Figure 10. EXAFS spectrum (left) and Fourier transform (right) of (a) chemically synthesized and purified $^{99}Tc^{V}O(\alpha_2\text{-}P_2W_{17}O_{61})^{7-}$ and (b) a 4 mM sample of α_2-$[P_2W_{17}O_{61}]^{10-}$ containing $^{99}TcO_4^-$ in 0.5 M of H_2SO_4, D_2O, and 2-propanol (2:1:1 vol), following exposure to sunlight for 2 months.

The EXAFS spectrum of the sample is shown in Figure 10b along with the EXAFS spectrum of a chemically synthesized, isolated, and purified **^{99}Tc^{V}O-α2**,[40] which is shown in Figure 10a for comparison. The ^{31}P NMR (Figure 9a) shows a significant resonance at −14.3 ppm, assigned to the ^{99}Tc/P containing intermediate, which persists in solution. Thus, the sample provides a reasonable model for employing EXAFS and XANES to understand the coordination and the oxidation state of the intermediate. The fitting parameters are given in Table 2.

The EXAFS data reveal that the sample contains both short and long Tc−O bonds as well as an interaction between ^{99}Tc and W atoms at 3.35 Å. Two Debye−Waller parameters are used for the model: the σ^2 of Tc═O is fixed at 0.002 Å^2, which is a typical value for a ^{99}Tc terminal oxo ligand, and the rest of the model uses a single Debye−Waller parameter for all shells. The fit of the model to the data is good though not perfect. As shown in Figure 10b, the Fourier transform contains two large peaks, which are well fit by the model; however, there are two small peaks between the main peaks that were not modeled (the large peak in the Fourier transform below 1 Å is an experimental artifact, which is not in the region being modeled and does not affect the fit). Attempts to fit these small peaks using O, S, P, Tc, or W neighbors did not improve the fit.

As is obvious from the Fourier transform in Figure 10, the local environment of ^{99}Tc in the photolytically reduced sample is reminiscent of the chemically synthesized **^{99}Tc^{V}O-α2**; however, significant differences exist between the spectra. First, the amplitude of the EXAFS spectrum of the photolytically reduced sample is significantly smaller than that of chemically synthesized **^{99}Tc^{V}O-α2**, which is largely due to greater disorder as expected for a sample that consists of a mixture of species. As a result of this disorder, the coordination numbers given in Table 2 have low precision. Second, the only W neighbors observed in the EXAFS spectrum of the sample containing the intermediate are those at 3.35 Å, which is significantly shorter than the shorter Tc−W distance in **^{99}Tc^{V}O-α2**, 3.42 Å. In addition, the W neighbors at 3.57 Å in **^{99}Tc^{V}O-α2** are not observed in the intermediate spectrum. These differences strongly suggest that the Tc−W distance in the intermediate is not due solely to the presence of **^{99}Tc^{V}O-α2**. In other words, ^{99}Tc is coordinated by the **α2** ligand in the intermediate as well as in the product. Unlike the coordination numbers, the Tc−W distances are precise, even in a mixture of species, and can be used to address the interaction between Tc and P_2W_{17} in the intermediate. The distance, 3.35 Å,

Table 2. EXAFS Fitting Parameters for the ^{99}Tc/P-Containing Intermediate

neighbor	no. of neighbors	distance (Å)	s^2 (Å^2)	p(F)[b]	distances in **Tc^{V}O-α2**
O	1.1(2)	1.728(6)	0.002[c]	<0.001	1.638(4)
O	4.0(8)	2.01(1)	0.008(2)	<0.001	1.996(4)
W	2.0(9)	3.35(2)	0.008(2)[d]	0.005	3.43(2)
O	6(3)	3.9(2)	0.008(2)[d]	0.038	3.97(2)

[a] $S_0^2 = 1$ (fixed), $DE_0 = 3(3)$ eV. [b] Probability that the improvement to the fit of including this shell is due to random error. [c] Fixed at 0.002. [d] Constrained to equal the Debye−Waller parameter of the second oxygen shell.

between the ^{99}Tc and W atoms in the intermediate is not consistent with monodentate coordination of ^{99}Tc to a single W atom, which would have a longer bond distance, ~4 Å, as well as significant enhancement of the EXAFS signal due to multiple scattering, neither of which is observed. Likewise, this distance is not consistent with ^{99}Tc coordinated by 4 W atoms of ***α*2**, which would produce a spectrum identical to **^{99}Tc^{V}O-*α*2**. The only plausible interaction between ***α*2** and ^{99}Tc that would result in a 3.35 Å Tc−W distance is a bidentate coordination of ^{99}Tc by two of the W−O sites of ***α*2**. The identities of the other ligands coordinated to ^{99}Tc cannot be determined except that the atom coordinated to ^{99}Tc must be O; coordination by either water or sulfate[75] is consistent with the EXAFS spectrum.

Discussion of Intermediate and Mechanism of ^{99}Tc and Re Incorporation. Reduction of $^{99}TcO_4^-$ in these experiments to ^{99}Tc(IV) is consistent with the XAS experiments and is chemically reasonable. First, electrochemical studies of the **^{99}Tc^{V}O-*α*2** show that the ^{99}Tc(IV) oxidation state is accessible and reversible.[40] Second, reduction of $^{99}TcO_4^-$ in the presence of poorly complexing ligands results in the $^{99}Tc^{IV}O_2 \cdot xH_2O$ that precipitates out as a black solid. In this study, however, ***α*2** and the ligands present in the reduction media (sulfate, decomposition products of 2-propanol, water) likely sequester ^{99}Tc(IV) as a mixed ligand−***α*2** complex, wherein two of the W−O of the lacunary site coordinate to the ^{99}Tc with the remainder of the coordination sphere taken up by other coordinating ligands that stabilize the intermediate complex. The amount of the intermediate complex increases when a stoichiometry of 1:1 ***α*2**:$^{99}TcO_4^-$ is employed in irradiation experiments, leading to a method for attempted isolation of the intermediate complex(es) and further study.

The well-known periodic comparisons of ^{99}Tc and Re provide an understanding of the differences in the reduction of MO_4^- (M = ^{99}Tc and Re) and complexation of the low-valent metal into the ***α*2** framework. The reduction of ^{99}Tc is more facile than that of Re; therefore, it is not surprising that the $^{99}TcO_4^-$ can be reduced to a ^{99}Tc(IV) intermediate, while ReO_4^- is reduced to Re(V) with no intermediate formation. Moreover, the ability of ReO_4^- to expand the Re coordination from 4 to 6 may be operative in this case.[68,70,71] Kinetic studies, monitoring polarographic-limiting current, conclude that the 1:1 ReO_4^-:citrate complex facilitates reduction to Re(V).[71] A close association (or complex) of ReO_4^- with the ***α*2** in the reduction media may facilitate reduction to Re(V) and fast incorporation into the ***α*2** vacancy. Such an association of anions may occur via solvent-separated or -shared anion−anion interactions. Also the association of anions may be mediated via cations or protons that are present in the solutions.

CONCLUSION

The contaminant, $^{99}TcO_4^-$, is a mobile oxyanion that is found in the groundwater and soils near national laboratory facility sites. Reduction of the ^{99}Tc(VII) and incorporation into materials to form stable reduced ^{99}Tc materials would facilitate remediation strategies. Presently, most efforts that have been tested for deployment in the field result in oxidation of the reduced ^{99}Tc (mostly ^{99}Tc(IV) in the form of $^{99}TcO_2$) back to $^{99}TcO_4^-$. Herein we introduce one material (the ***α*2** Wells−Dawson POM) to both reduce the $^{99}TcO_4^-$ and incorporate the reduced ^{99}Tc covalently into the bonds of the material. An advantage of our study is that we can identify the product on the molecular level and thereby address the process of metal reduction and incorporation.

The lacunary ***α*2** Wells−Dawson POM is photoactivated by light and reduced by two electrons donated by a sacrificial electron donor (2-propanol). The reduced α_2-$P_2W_{17}O_{61}^{12-}$ efficiently transfers electrons to $^{99}TcO_4^-$ (and ReO_4^-), and the reduced $^{99}Tc^{V}$ (Re^{V}) is incorporated into the reoxidized ***α*2** as **^{99}Tc^{V}O-*α*2** (and **Re^{V}O-*α*2**). Addition of MO_4^- (M = ^{99}Tc, Re) to reduced α_2-$P_2W_{17}O_{61}^{12-}$, probed by ^{31}P NMR, radio TLC, and observation of rest potential, all as a function of time, shows that the reduction of MO_4^- is rapid in both cases, but in the case of ^{99}Tc, a ^{99}Tc/P-containing intermediate is formed. This intermediate then slowly converts to the **^{99}Tc^{V}O-*α*2** product. EXAFS and XANES analysis suggests that the intermediate consists of a ^{99}Tc(IV) oxo species bound to two oxygen atoms of the four W−O in the ***α*2** defect. The other coordination sites may be taken up by sulfate, water, or other entities, such as decomposition products of the 2-propanol.

The Re does not go through an intermediate and possesses faster kinetics to produce the **Re^{V}O-*α*2** product. This may be ascribed to the potential of ReO_4^- for expansion of coordination sphere to form a ReO_4^- complex with the ***α*2**. As seen in early studies, such a ReO_4^- complex may facilitate electron transfer to form the **Re^{V}O-*α*2** complex. This study illustrates the sometimes significant differences between the chemistry of technetium and rhenium and second and third row congeners.

Reduction of $^{99}TcO_4^-$ mediated by photoactivated ***α*2** to form **^{99}Tc^{V}O-*α*2** can also be accomplished in sunlight. While the sunlight reactions are not as efficient as employing a continuous irradiation source, the fact that this process works to form exclusively product is encouraging. Other POMs or other materials with absorbances in the visible region may be more appropriate when using sunlight as a photoactivation source.

This study opens the door for the use of metal oxide materials for reduction of $^{99}TcO_4^-$ and incorporation of the reduced ^{99}Tc covalently into the material. Moreover, POMs may provide a suitable platform to study the molecular level dynamics and mechanisms of the reduction of $^{99}TcO_4^-$ and incorporation of the reduced ^{99}Tc into a material.

ASSOCIATED CONTENT

Supporting Information. Figures: radio TLC data for ^{99}Tc and ^{188}Re, ^{31}P NMR data monitoring speciation as a function of time for 8 mM and 16 mM POM concentrations; stability data of the ***α*2** ligand at pH 0.33 as a function of concentration and time; the control Absorbance spectra of $^{99}TcO_4^-$ in 0.5 mM H_2SO_4: D_2O: 2-propanol (2:1:1 vol.) at pH 0.33; calculations correlating ^{31}P NMR with radio TLC; ^{99}Tc NMR showing speciation of Tc; rest potential profile in electrolysis experiments for ^{99}Tc and Re; UV-Visible spectra, XANES spectra of intermediate. Supporting tables include ^{31}P NMR data and results from fitting the Tc K-edge XANES spectrum of the Tc/P intermediate. This material is available free of charge via the Internet at http://pubs.acs.org.

AUTHOR INFORMATION

Corresponding Author
lfrances@hunter.cuny.edu

Present Addresses
‖ Institut Lavoisier, UMR8180, Université de Versailles St. Quentin, 45 Avenue des Etats-Unis, 78035 Versailles Cedex, France

■ ACKNOWLEDGMENT

We are grateful to the NSF (grant nos. CHE 0414218 and CHE 0750118), the Office of Science (BER) —U.S. Department of Energy (DOE) (Award DE-SC0002456) and to DE-FG02-09ER16097 (Heavy Element Chemistry, Office of Basic Energy Sciences of the U.S. Department of Energy for support of this work. We are also grateful to Dr. Ghada Al Kadamany for critical analysis of our work. Research infrastructure at Hunter College is partially supported by Grant Number RR003037 from the National Center for Research Resources (NCRR), a component of the National Institutes of Health (NIH). Part of this work was performed at Lawrence Berkeley National Laboratory and was also supported by Heavy Element Chemistry, Office of Science, Office of Basic Energy Sciences of the U.S. DOE under contract no. DE-AC02-05CH11231. EXAFS data were obtained at the Stanford Synchrotron Radiation Laboratory, a national user facility operated by Stanford University on behalf of the Office of Basic Energy Sciences, U.S. DOE.

■ REFERENCES

(1) Lukens, W. W.; Shuh, D. K.; Schroeder, N. C.; Ashley, K. R. *Environ. Sci. Technol.* **2004**, *38*, 229.
(2) Burke, I. T.; Boothman, C.; Lloyd, J. R.; Livens, F. R.; Charnock, J. M.; McBeth, J. M.; Mortimer, R. J. G.; Morris, K. *Environ. Sci. Technol.* **2006**, *40*, 3529.
(3) Burke, I. T.; Boothman, C.; Lloyd, J. R.; Mortimer, R. J. G.; Livens, F. R.; Morris, K. *Environ. Sci. Technol.* **2005**, *39*, 4109.
(4) Liu, Y.; Terry, J.; Jurisson, S. *Radiochim. Acta.* **2008**, *96*, 823.
(5) Lloyd, J. R.; Sole, V. A.; Van Praagh, C. V. G.; Lovley, D. R. *Appl. Environ. Microbiol.* **2000**, *66*, 3743.
(6) Lukens, W. W.; Bucher, J. J.; Shuh, D. K.; Edelstein, N. M. *Environ. Sci. Technol.* **2005**, *39*, 8064.
(7) Maes, A.; Geraedts, K.; Bruggeman, C.; Vancluysen, J.; Rossberg, A.; Henning, C. *Environ. Sci. Technol.* **2004**, *38*, 2044.
(8) Stalmans, M.; Maes, A.; Cremers, A. In *Technetium in the Environment*; Desmet, G., Myttenaere, C., Eds.; Elsevier Applied Sciemce Publishers Ltd.: Essex, England, 1986, p 91.
(9) Van Loon, L.; Stalmans, M.; Maes, A.; Cremers, A.; Cogneau, M. In *Technetium in the Environment*; Desmet, G., Myttenaere, C., Eds.; Elsevier: 1986, p 143.
(10) Wildung, R. E.; Li, S. W.; Murray, C. J.; Krupka, K. M.; Xie, Y.; Hess, N. J.; Roden, E. E. *FEMS Microbiology Ecology* **2004**, *49*, 151.
(11) Vance, E. R.; Hart, K. P.; Carter, M. L.; Hambley, M. J.; Day, R. A.; Begg, B. D. In *Materials Research Society Symposium Proceedings Scientific Basis for Nuclear Waste Management XXI*; Materials Research Society: Warrendale, PA, 1998; Vol. 506, p 289.
(12) Balogh, J. C.; Grigal, D. F. *Soil Science* **1980**, *130*, 278.
(13) Sekine, T.; Watanabe, A.; Yoshihara, K.; Kim, J. I. *Radiochim. Acta.* **1993**, *63*, 87.
(14) Istok, J. D.; Senko, J. M.; Krumholz, L. R.; Watson, D.; Bogle, M. A.; Peacock, A.; Chang, Y. J.; White, D. C. *Environ. Sci. Technol.* **2004**, *38*, 468.
(15) Wellman, D. M.; Mattigod, S. V.; Parker, K. E.; Heald, S. M.; Wang, C.; Fryxell, G. E. *Inorg. Chem.* **2006**, *45*, 2382.
(16) Geletii, Y. V.; Hill, C. L.; Bailey, A. J. H., K.I.; Atalla, R. H.; Weinstock, I. A. *Inorg. Chem.* **2005**, *44*, 8955.
(17) Mandal, S.; Mandale, A. B.; Sastry, M. *J. Mater. Chem.* **2004**, *14*, 2868.
(18) Mandal, S.; Rautaray, D.; Sastry, M. *J. Mater. Chem.* **2003**, *13*, 3002.
(19) Mandal, S.; Selvakannan, P. R.; Pasricha, R.; Sastry, M. *J. Am. Chem. Soc.* **2003**, *125*, 8440.
(20) Papaconstantinou, E.; Hiskias, A.; Troupis, A. *Front. Biosci.* **2003**, *8*, S813.
(21) Pope, M. T.; Varga, G. M. *Inorg. Chem.* **1966**, *5*, 1249.
(22) Sadakane, M.; Steckhan, E. *Chem. Rev.* **1998**, *98*, 219.
(23) Grika, E.; Troupis, A.; Hiskia, A.; Papaconstantinou, E. *Environ. Sci. Technol.* **2005**, *39*, 4242.
(24) Hiskia, A.; Mylonas, A.; Papaconstantinou, E. *Chem. Soc. Rev.* **2001**, *30*, 62.
(25) Hiskia, A.; Troupis, A.; Antonaraki, S.; Gkika, E.; Papaconstantinou, P. K. *Int. J. Environ. Anal. Chem.* **2006**, *86*, 233.
(26) Hiskia, A.; Troupis, A.; Papaconstantinou, E. *Int. J. Photoenergy* **2002**, *4*, 35.
(27) Ioannidis, A.; Papaconstantinou, E. *Inorg. Chem.* **1985**, *24*, 439.
(28) Papaconstantinou, E. *Chem. Soc. Rev.* **1989**, *18*, 1.
(29) Troupis, A.; Gkika, E.; Hiskia, A.; Papconstantinou, E. *C. R. Chim.* **2006**, *9*, 851.
(30) Troupis, A.; Hiskia, A.; Papaconstantinou, E. *New J. Chem.* **2001**, *25*, 361.
(31) Troupis, A.; Hiskia, A.; Papaconstantinou, E. *Angew. Chem., Int. Ed.* **2002**, *41*, 1911.
(32) Troupis, A.; Triantis, T. M.; Gkika, E.; Hiskia, A.; Papaconstantinou, E. *Appl. Catal., B* **2009**, *86*, 98.
(33) Gordeev, A. V.; Kartashev, N. I.; Ershov, B. G. *High Energy Chem.* **2002**, *36*, 75.
(34) Keita, B.; Mbomekalle, I. M.; Lu, Y. W.; Nadjo, L.; Berthet, P.; Anderson, T. M.; Hill, C. L. *Eur. J. Inorg. Chem.* **2004**, *17*, 3462.
(35) Li, H.; Yang, Y.; Wang, Y.; Li, W.; Bi, L.; Wu, L. *Chem. Commun. (Cambridge, U. K.)* **2010**, *46*, 3750.
(36) Zhang, G.; Xu, Y. *Inorg. Chem. Commun.* **2005**, *8*, 520.
(37) Keita, B.; Liu, T.; Nadjo, L. *J. Mater. Chem.* **2009**, *19*, 19.
(38) Finke, R. G. *Transition Metal Nanoclusters: solution-phase synthesis, then characterization and mechanism of formation, of polyoxoanion-and tetrabutylammonium-stabilized nanoclusters*; Marcel Dekker, Inc: New York, 2001.
(39) Lin, Y.; Finke, R. G. *J. Am. Chem. Soc.* **1994**, *116*, 8335.
(40) McGregor, D.; Burton-Pye, B. P.; Howell, R. C.; Mbomekalle, I. M.; Wayne W. Lukens, J.; Bian, F.; Mausolf, E.; Poineau, F.; Czerwinski, K. R.; Francesconi, L. C. *Inorg. Chem.* **2011**, *50*, 1670.
(41) Libson, K.; Woods, M.; Sullivan, J.; Watkins, J. W., II; Elder, R. C.; Deutsch, E. *Inorg. Chem.* **1988**, *27*, 999.
(42) Vanderheyden, J.; Ketring, A.; Libson, K.; Heeg, M.; Roecker, L.; Motz, P.; Whittle, R.; Elder, R. C.; Deutsch, E. *Inorg. Chem.* **1984**, *23*, 3184.
(43) Boyd, G. E. *J. Chem. Educ.* **1959**, *36*, 3.
(44) Davison, A.; Trop, H.; DePamphilis, B.; Jones, A. *Inorg. Synth.* **1982**, *21*, 160.
(45) Contant, R. *Inorg. Synth.* **1990**, *27*, 71.
(46) Venturelli, A.; Nilges, M. J.; Smirnov, A.; Belford, R. L.; Francesconi, L. C. *J. Chem. Soc., Dalton Trans.* **1999**, 301.
(47) Keita, B.; Girard, F.; Nadjo, L.; Contant, R.; Belghiche, R.; Abessi, M. *J. Electroanal. Chem.* **2001**, *508*, 70.
(48) Berning, D. E.; Schroeder, N. C.; Chamberlin, R. M. *J. Radioanal. Nucl. Chem.* **2005**, *263*, 613.
(49) Bard, A. J.; Parsons, R.; Jordan, J. *Standard Potentials in Aqueous Solution*; Marcel Dekker, Inc.: New York, 1985.
(50) Bratsch, S. G. *J. Phys. Chem. Ref. Data* **1989**, *18*, 1.
(51) Fox, M. A.; Cardona, R.; Gaillard, E. *J. Am. Chem. Soc.* **1987**, *109*, 6347.
(52) Newville, M. J. *Synchrotron Rad* **2001**, *8*, 322.
(53) Ravel, B. *Phys. Scr.* **2005**, *T115*, 1007.
(54) Rehr, J. J.; Albers, R. C.; Zabinsky, S. I. *Phys. Rev. Lett.* **1992**, *69*, 3397.
(55) D'Amour, V. H. *Acta Crystallogr.* **1976**, *B32*, 729.
(56) Bevington, P. R.; Robinson, K. D. *Data Reduction and Error Analysis for the Physical Sciences*; McGraw-Hill: Boston, MA, 1992.
(57) Downward, L.; Booth, C. H.; Lukens, W. W.; Bridges, F. *AIP Conf. Proc.* **2007**, *882*, 129.
(58) Antonaraki, S.; Triantis, T. M.; Papaconstantinou, E.; Hiskia, A. *Catal. Today* **2010**, *151*, 119.
(59) Choi, W. *Prepr. Ext. Abstr.—ACS Natl. Meet., Am. Chem. Soc., Div. Environ. Chem.* **2006**, *46*, 400.

(60) Ettedgui, J.; Diskin-Posner, Y.; Weiner, L.; Neumann, R. *J. Am. Chem. Soc.* **2011**, *133*, 188.
(61) Jin, H.; Wu, Q.; Pang, W. *J. Hazard. Mater.* **2007**, *141*, 123.
(62) Kormali, P.; Troupis, A.; Triantis, T.; Hiskia, A.; Papaconstantinou, E. *Catal. Today* **2007**, *124*, 149.
(63) Li, H.; Pang, S.; Feng, X.; Muellen, K.; Bubeck, C. *Chem. Commun. (Cambridge, U. K.)* **2010**, *46*, 6243.
(64) Li, H.; Pang, S.; Wu, S.; Feng, X.; Mullen, K.; Bubeck, C. *J. Am. Chem. Soc.* **2011**, *133*, 9423.
(65) Liu, L.; Wang, L.-m.; Chu, D.-q. *Adv. Mater. Res. (Zuerich, Switz.)* **2010**, *113*−*116*, 2045.
(66) Radivojevic, I.; Burton-Pye, B. P.; McGregor, D.; Mbomekalle, I. M.; Lukens, W. W.; Francesconi, L. C., **2011**, in preparation.
(67) Kozik, M.; Baker, L. C. W. *J. Am. Chem. Soc.* **1990**, *112*, 7604.
(68) *The inorganic chemistry of technetium and rhenium as relevant to nuclear medicine*; Deutsch, E., Libson, K., Vanderheyden, J.-L., Eds.; Cortina International: Verona, Italy, 1990; Vol. 3.
(69) Libson, K.; Helm, L.; Roodt, A.; Cutler, C.; Merbach, A. E.; Sullivan, J. C.; Deutch, E. *Kinetics and mechanism of ligand substitution on analogous technetium(V) and rhenium(V) complexes*; 3rd ed.; Cortina International: Verona, Italy, 1989.
(70) Murmann, R. K. *J. Phys. Chem.* **1967**, *71*, 974.
(71) Vajo, J. J.; Aikens, D. A.; Ashley, L.; Poeltl, D. E.; Bailey, R. A.; Clark, H. M.; Bunce, S. C. *Inorg. Chem.* **1981**, *20*, 3328.
(72) McGregor, D.; Burton-Pye, B. P.; Mbomekalle, I. M.; Lopez, X.; Romo, S.; Poblet, J.-M.; Francesconi, L. C., **2011**, in preparation.
(73) Biboum, R. N.; Njiki, C. P. N.; Zhang, G.; Kortz, U.; Mialane, P.; Dolbecq, A.; Mbomekalle, I. M.; Nadjo, L.; Keita, B. *J. Mater. Chem.* **2011**, *21*, 645.
(74) Fay, N.; Hultgren, V. M.; Wedd, A. G.; Keyes, T. E.; Forster, R. J.; Leane, D.; Bond, A. M. *Dalton Trans.* **2006**, 4218.
(75) Vichot, L.; Fattahi, M.; Musikas, C.; Grambow, B. *Radiochim. Acta.* **2003**, *91*, 263.